Viscoelasticity of Adsorbed Polymer Layers

P. Sens,* C. M. Marques, and J. F. Joanny

Institut Charles Sadron, 6 rue Boussingault, 67083 Strasbourg Cedex, France

Received December 17, 1993; Revised Manuscript Received March 23, 1994•

ABSTRACT: We discuss theoretically dynamic measurements with a surface force apparatus composed of a plane and a sphere coated with adsorbed polymer layers in a good solvent. The hydrodynamics are studied within a simple two fluids model where the friction between polymer and solvent is described by the so-called Brinkman approximation. In a steady compression experiment the distance between the sphere and the plane varies at a constant velocity and the polymer layers have a hydrodynamic thickness e_H of the order of their radius of gyration. In a periodic compression experiment, the distance has a periodic modulation of small amplitude at a finite frequency; the results are recast in terms of a complex modulus G. At a low frequency, the modulus has the standard Maxwell behavior ($G' \simeq \omega^2$, $G'' \simeq \omega$). The contribution of the polymer to the loss modulus G'' is small when the polymer layers do not overlap; it is of the same order of magnitude as the pure solvent contribution when they do overlap. The elastic modulus increases with the thickness of the adsorbed layers. At a high frequency, the complex modulus increases as $G \simeq \omega^{2/3}$ and is independent of the thickness of the polymer layers. When the adsorbed polymer layers overlap, there is an intermediate regime where the elastic part of the modulus increases as $G' \simeq \omega^{4/3}$.

1. Introduction

The interactions between surfaces coated with adsorbed polymers have been the subject of extensive studies because of their major role in the stabilization of highly concentrated colloidal solutions. Recent advances in the experimental studies of these interactions have been made possible by the development of the surface force apparatus initiated by Israelachvili and Tabor.[1] This apparatus measures directly the force between two mica plates separated by a thin liquid film at a well-controlled distance of the order of a few angstroms. Both static and dynamic forces between plates can be measured. When the thin liquid film is a polymer layer adsorbed from a good solvent, the *static force* has a repulsive component due to the change of the chains osmotic pressure when the gap thickness varies and an attractive component due to the gridging between the two surfaces by the long polymer chains. The relative importance of these two components is well understood and has been studied in great details by the group of Klein.[2,3] The *dynamic force* vanishes in the absence of relative motion of the plates and has a hydrodynamic origin. For a Newtonian fluid, it is given by Reynolds lubrication theory:[4,5] if the two plates are a plane and a sphere of radius R (of the order of 1 cm), the dynamic force is repulsive and equal to:

$$F = -6\pi R^2 \frac{\eta}{h_0} \dot{h}_0 \tag{1}$$

where $h_0(t)$ is the minimum distance between the sphere and the plane, η the viscosity of the fluid, and the dot indicates a derivative with respect to time.

The aim of this paper is to consider theoretically the equivalent of the Reynolds equation for a polymer solution. We consider the case where polymer is irreversibly adsorbed on the solid surfaces from a good solvent and where the bulk solution is then washed and replaced by pure solvent. The total amount of polymer per unit area Γ adsorbed on the solid surface is fixed. We also assume that the polymer moves slowly and does not have time to desorb during compression. When the adsorption is done at saturation, the static force between the solid surfaces induced by the polymer is repulsive. If the surfaces are far enough apart, the dynamic repulsion is well described by Reynolds theory (eq 1), after correcting h_0 by the polymer layer hydrodynamic thickness. The hydrodynamic thickness is of the order of the Flory radius R_f of the polymer chains (In a good solvent, the Flory radius increases with the degree of polymerization N as $R_f \propto N^{3/5}$). When the distance between the plates is smaller than the Flory radius R_f, the dynamic force is the sum of an "in phase" elastic repulsion due to the elasticity of the adsorbed layers of an "out of phase" lubrication force which includes the viscous friction of the solvent on the polymer.

Experiments in this geometry have been recently performed by Pelletier et al.[6] An oscillatory motion has been imposed on a sphere-plane apparatus normal to the plane, and the dynamical response of an adsorbed polymer solution has been measured as a function of frequency.

The viscoelastic response of the complex polymeric fluid to oscillatory squeezing is characterized by the shear relaxation modulus $G(t)$, which links the shear stress $\sigma(t)$ to the shear strain $\gamma(t)$:[7]

$$\sigma(t) = \int_{-\infty}^{t} dt' G(t - t') \dot{\gamma}(t') \tag{2}$$

In Fourier space, one defines the complex modulus $G^*(\omega) = G'(\omega) + iG''(\omega)$ by

$$G^*(\omega) = i\omega\eta + i\omega \int_0^\infty dt\, e^{-i\omega t} G^{(p)}(t) \tag{3}$$

where η is the solvent viscosity and $G^{(p)}$ the polymer contribution to the modulus $G(t)$. The real part $G'(\omega)$ is the storage modulus ("in phase"-response) and the imaginary part $G''(\omega)$ is the loss modulus.

The force acting on one plate when the other one moves is related to the modulus by

$$F(t) = -6\pi R^2 \int_{-\infty}^{t} dt'\, G(t - t') \dot{\gamma}(t'),$$

$$F(\omega) = -6\pi R^2 \gamma G^*(\omega) \tag{4}$$

where the factor $-6\pi R^2\gamma$ has been introduced by analogy with the Reynolds formula: the loss modulus of a periodically compressed newtonian fluid if $G''(\omega) = \eta(\dot{h}_0/h_0) = i\omega\eta$.

As depicted in Figure 1, our (theoretical) surface force apparatus is composed of a fixed plane and an oscillating sphere of radius R. The mean separation between the

• Abstract published in *Advance ACS Abstracts*, June 1, 1994.

0024-9297/94/2227-3812$04.50/0

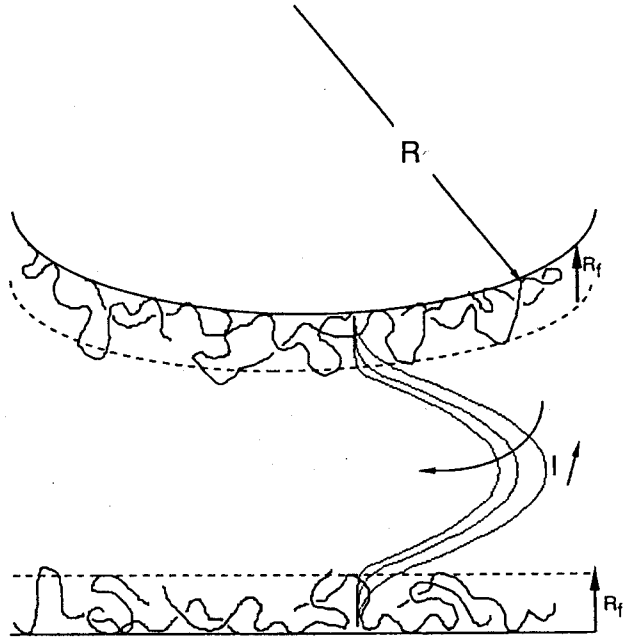

Figure 1. Second-order velocity profile in the nonoverlapping geometry ($R_f < h_0/2$). The profile is plotted for three different values of the friction parameter l: $l = 3$, $l = 5$, $l = 10$.

surfaces varies along the radial coordinate $\mathbf{r}$ as $h(r) \simeq h_0 + r^2/2R$ if $R \gg h_0$ where h_0 is the smallest distance between the surfaces.

In the following, we consider two different types of compression: steady squeezing with a constant (small) velocity difference between the plates, and oscillatory squeezing, where the upper plate has small oscillations around its mean position, with a shear strain $\gamma(t)$. The time-dependent thickness is $h(r,t) = h(r) + h_0\gamma(t)$.

The spirit of our calculation is similar to that of Fredrickson and Pincus[8] for compressed grafted polymer layers. In this approach, the chains are considered as an elastic porous medium through which the solvent flows. The friction between the solvent and the polymers induces an extra viscous dissipation and an elastic deformation of the network formed by the polymer chains. The main difference between the two problems lies in the polymer density profile. The concentration profile in a grafted layer varies smoothly and can be approximated by a constant (a more accurate description is a parabolic profile). In an adsorbed layer, the concentration profile decays as a power law of the distance from the adsorbing surface. In order to describe in a simple manner the polymer concentration in the adsorbed layers, we use the scaling picture introduced by de Gennes[9] where an adsorbed polymer layer is described as a self-similar grid. In a good solvent a polymer solution has a correlation length of the order of the mesh size of the temporary network formed by the chains, that decays with the bulk concentration as $\xi(c) \propto c^{-3/4}$.[10] In the scaling analysis, the adsorbed layer is considered locally as a semidilute solution which becomes denser in the vicinity of the adsorbing surface. The solution has locally no characteristic length scale and the local correlation length must be proportional to the distance to the wall $\xi(z) \simeq z$. The concentration varies then as $c(z) \simeq z^{-4/3}$. In the case where the adsorbed layers on the two plates are not overlapping, the two adsorbed layers are independent and the self-similar concentration profile is cut at a distance from the adsorbing surface equal to the size of the largest loops, i.e. at a distance of the order of the Flory radius. When the two adsorbed layers are moderately overlapping, we can use the Derjaguin approximation according to our hypothesis of large sphere radius.[1] We consider the two plates to be locally parallel and assume that the concentration profile is self-similar on each adsorbing surface and symmetric with respect to the midplane.

The paper is organized as follows. In the next section we introduce the general framework of the two fluids model and the lubrication approximation that allows the derivation of the viscoelasticity of the adsorbed polymer layer. Section 3 studies nonoverlapping polymer layers. We first discuss steady compression and then oscillatory compression in the limit of low pulsation ω where the internal modes of the adsorbed polymer loops do not contribute to the viscoelasticity. This is the case when $\omega\tau_R < 1$ where τ_R is the Zimm relaxation time of the largest loops with a size of the order of the Flory radius of the chains[11] ($\tau_R \propto \eta R_f^3/k_BT \propto \eta(aN^{3/5})^3/k_BT$). Overlapping layers are considered in section 4 and oscillatory compression at high frequency is briefly studied in section 5. The last section presents some concluding remarks and comparisons with experiments.

2. Two Fluids Model

The viscoelastic properties of the confined solution are described within the framework of a two fluids hydrodynamic model. The two fluids are the solvent considered as a Newtonian fluid and the network formed by the adsorbed polymer loops. The displacement of the sphere induces a pressure gradient in the radial direction $\mathbf{r}$ and a radial flow of solvent. The drag of the fluid through the network then creates viscous dissipation and an elastic strain of the polymer. The drag is described here by the Brinkman equation,[12] that approximates the polymer solution by a porous medium with a permeability of order η/ξ^2. The hydrodynamic equation for the solvent flow is the Stokes equation:

$$\eta\nabla^2\mathbf{v} - \frac{\eta}{\xi_n^2}(\mathbf{v} - \dot{\mathbf{u}}) - \nabla P = 0 \tag{5}$$

where $\mathbf{v}$ and $\mathbf{u}$ are the solvent velocity field and the polymers displacement field. The first term is the viscous stress, and the last one the pressure gradient. The second term describes the friction between polymer and solvent in the Brinkman approximation. The permeability has here been written as η/ξ_n^2 where ξ_n is a length proportional to the local correlation length ξ. Since in each adsorbed layer the correlation length is proportional to the distance to the adsorbing surface z, it is convenient to define a dimensionaless number l such that $\xi_n^{-2} = l(l-1)/z^2$ if $z < h/2$ and $\xi_n^{-2} = l(l-1)/(h-z)^2$ if $z > h/2$. The number l measures the friction of the solvent of the polymer and is larger than 1 (if $l = 1$ the friction vanishes). This number is mainly dependent on the quality of the solvent. The equation of motion of the polymer is a balance between the elastic stress in the solvent and the friction force:

$$\nabla(E(z)\nabla\mathbf{u}) + \frac{\eta}{\xi_n^2}(\mathbf{v} - \dot{\mathbf{u}}) = 0 \tag{6}$$

where $E(z)$ is the local Young modulus of the polymer solution which in a scaling approach is proportional to the osmotic pressure $E(z) \simeq k_bT/\xi^3(z) = \alpha k_bT/z^3$ where α is a numerical constant.

Locally the adsorbed polymer layer can be considered as an isotropic elastic medium and is characterized by two elastic moduli, the Lamé coefficients. At the level of scaling arguments, it can be argued that the two elastic moduli have the same scaling behavior with the local concentration and that the Poisson ratio is a number independent of the

polymer concentration. Following Fredrickson and Pincus, we have introduced here only the shear modulus and we have implicitly assumed that the Poisson ratio vanishes. It is shown at the end of section 3 that except at very low frequency, the contribution to the elastic stress considered here is dominant even for incompressible layers.

In the case of steady squeezing with slow displacement of the upper plate, the polymer has time to relax toward its equilibrium configuration; we thus only need to consider the motion of the solvent through a fixed netweork ($\mathbf{u} = 0$). If the squeezing is obtained by an oscillatory motion of the plates, the displacement of the polymer network has to be taken into account. Equations 5 and 6 are then coupled.

In the case where the distance between the sphere and the plane h is much smaller than the radius of the sphere, the two fluids model can be further simplified by using the lubrication approximation.[5] The typical length scale for the variation of the velocity in the z direction is much smaller than the typical length scale in the radial direction. This imposes that the velocity is essentially radial ($v_z \ll v_r$) and that the pressure does not depend on the transverse coordinate z; the pressure gradient is also radial. The equations of motion in this approximation reduce to

$$\eta\partial_z^2 v_r - \eta\frac{l(l-l)}{z^2}(v_r - \dot{u}_r) - \partial_r P = 0 \tag{7}$$

$$\partial_z\left(\frac{\alpha k_B T}{z^3}\partial_z u_r\right) + \eta\frac{l(l-1)}{z^2}(v_r - \dot{u}_r) = 0 \tag{8}$$

The solvent imcompressibility equation can be written as $\nabla\mathbf{v} = 0$ or $\partial_z v_z = -(1/r)\partial_r(rv_r)$.

This allows a determination of the motion of the upper plate from the velocity field:

$$v_z(h) = h_0\dot{\gamma} = \int_0^h \partial_z v_z \mathrm{d}z = -\frac{2}{r}\partial_r\left(r\int_0^{\frac{h}{2}} v_r \mathrm{d}z\right) \tag{9}$$

we thus obtain

$$\int_0^{h/2} v_r \mathrm{d}z = -\frac{1}{4}\dot{\gamma}h_{0r} \tag{10}$$

The velocity field and the displacement field are obtained by integration of the coupled eqs 7 and 8 for a given pressure gradient. The pressure gradient is then derived from the continuity eq 10, and the hydrodynamic force is obtained by integration of the stress tensor over the radial surface:

$$F = \int_0^\infty 2\pi r\mathrm{d}r(P(r) - P_\infty - 2\eta\partial_z v_z|_{z=0}) = 2\pi R\int_{h_0}^\infty \mathrm{d}h(P(r) - P_\infty - 2\eta\partial_z v_z|_{z=0}) \tag{11}$$

The complex modulus is finally obtained from eq 4.

The *hydrodynamic* force is due to the drag of fluid on the polymer network. However this is not the only force between the sphere and the plane induced by the adsorbed polymer. There is a static force arising from the overlap of the two adsorbed layers. At a given spacing between the sphere and the plane, this force is compensated by the spring of the surface force apparatus and is thus not observable in a dynamic experiment. It is directly proportional to the osmotic pressure of the polymer solution at the middle of the gap. In a semidilute polymer solution, the osmotic pressure scales as:[9]

$$\Pi_{osm} = k_B T/\xi^3(z) \tag{12}$$

and the static force:

$$F_s \propto 2\pi\int_0^{r_l}\frac{k_B T}{\xi^3(h_0/2)}r\mathrm{d}r \tag{13}$$

The variation of the static force with the distance between plates gives rise to a finite contribution to the storage modulus G' at zero frequency. Note that the static force and thus the zero frequency limit of the storage modulus vanish in the limit where the two adsorbed polymer layers do not overlap. At a finite frequency, the force between the plates also has a contribution from the normal component of the elastic stress of the polymer network:

$$F_N = -2\pi R\int_{h_0}^\infty E(z=0)\partial_z u_z|_{z=0}\mathrm{d}h \tag{14}$$

In the limit where the curvature of the sphere is small, this elastic force and the component of the hydrodynamic force coming from the viscous stress tensor ($\eta\partial_z v_z$) can be neglected against the pressure contribution.

The Brinkman description of the hydrodynamics of the adsorbed polymer layers is valid only in the low frequency limit where the internal modes of the loops are not excited so that the adsorbed polymer layers can be considered as a porous medium. This requires that $\pi\tau_R < 1$ where τ_R is the Zimm relaxation time of the largest loops with a size of the order of the Flory radius. This low frequency limit seems to be the most relevant for the experimental results of Pelletier et al. The higher frequency limit is discussed briefly in section 6.

3. Nonoverlapping Polymer Layers

A. Steady Compression. When the distance between the sphere and the plane in the surface force apparatus decreases at a constant slow velocity, the polymer has time to relax toward its equilibrium conformation and there is no elastic strain. We discuss here the case where the two adsorbed polymer layers do not overlap ($R_f/h_0 < 1$).

We separate the gap between the sphere and the plane into three regions, two adsorbed layers of thickness R_F and the free solvent in between. The velocity field is found in each of these regions from eq 5 with an elastic deformation $\mathbf{u} = 0$. The viscous friction between polymer and solvent is finite in the adsorption layers but vanishes in the free solvent. At the boundaries between the adsorbed polymer and the free solvent ($z = R_f$), the radial velocity v_r and the transverse viscous stress $\partial_z v_r$ are continuous. The boundary conditions for the hydrodynamic motion are the no-slip condition on the walls $v_r(z = 0) = 0$ and the vanishing stress at the midplane $\partial_z v^s|_{h(r)/2} = 0$ (for symmetry reasons). We find inside the layers ($0 < z < R_f$)

$$v_r(z) = \frac{\partial_r P}{(l+1)(2-l)\eta}\left\{z^2 - \left((l-1)R_f^{2-l} + \frac{(l+1)(2-l)}{2l}h(r)R_f^{1-l}\right)z^l\right\} \tag{15}$$

and between the layers

$$v_r(z) = \frac{\partial_r P}{\eta}\left\{\frac{1}{2}(z^2 - h(r)z) + \frac{l-1}{2l}h(r)R_f - \frac{l-1}{2(l+1)}R_f^2\right\} \quad (16)$$

The dynamic force between the sphere and the plane is then calculated form the velocity field using the procedure detailed in the previous section.

$$F = -6\pi R^2\eta\frac{\dot{h}}{h_0}\left[1 + \frac{2(l-1)R_F}{l\ h_0} + O\left(\frac{R_f}{h_0}\right)^2\right] \quad (17)$$

If we introduce the hydrodynamic thickness of the adsorbed polymer layers as $e_H \simeq R_f[(l-1)/l]$, this force can be recast in the form of a Reynolds lubrication force as

$$F = -6\pi R^2\eta\frac{\dot{h}}{h_0 - 2e_H} \quad (18)$$

The friction of the solvent on the adsorbed polymer is thus equivalent to an effective reduction of the distance h_0 between the sphere and the plane by the hydrodynamic thickness of the adsorbed layers. This is in agreement with the result of deGennes for the flow along a wall coated with adsorbed polymer.[13]

B. Periodic Compression. We now study the periodic compression of the surface force apparatus when the two polymer layers are nonoverlapping at low frequency. The two adsorbed polymer layers constitute only a small perturbation, and the complex modulus is dominated by the loss modulus which has a value close to that of the pure solvent $G''(\omega) = \omega\eta$. The storage modulus $G'(\omega)$ is a correction of higher order in ω.

It is convenient from now on to use dimensionless units $\tilde{z} = z/h(r)$, $\tilde{u} = u_r/h(r)$ and $\tilde{t} = t/\tau(h)$ where we use the local thickness $h(r)$ as the unit length and the Zimm relaxation time of a loop of size $h(r)$, $\tau(h) = \eta h^3(r)/\alpha k_B T$ as the unit time. The pressure gradient is normalized as $B(h) = \partial_r P\tau(h)h(r) = \partial_r P h^4(r)/\alpha k_B T$.

For an oscillation of pulsation ω, we obtain the following equations of motion.

In the pure solvent ($\tilde{R}_f = R_f/h(r) < \tilde{z} < 1/2$):

$$\partial_{\tilde{z}}^2\tilde{v} = B(h) \quad (19)$$

In the polymers layers ($0 < \tilde{z} < \tilde{R}_f$)

$$\partial_{\tilde{z}}^2\tilde{v} - \frac{l(l-1)}{\tilde{z}^2}(\tilde{v} - i\omega\tau\tilde{u}) - B(h) = 0 \quad (20)$$

and

$$\partial_{\tilde{z}}\left(\frac{1}{\tilde{z}^3}\partial_{\tilde{z}}\tilde{u}\right) + \frac{l(l-1)}{\tilde{z}^2}(\tilde{v} - i\omega\tau\tilde{u}) = 0 \quad (21)$$

On the solid surfaces, the solvent velocity vanishes due to the no-slip boundary condition, and the polymer network is not deformed so that $\tilde{v}(\tilde{z} = 0) = \tilde{u}(\tilde{z} = 0) = 0$. At the edge of the adsorbed polymer layers, there is no stress on the polymer network and the elastic stress vanishes $\partial_{\tilde{z}}\tilde{u}|_{\tilde{R}_f} = 0$; the velocity and the transverse viscous stress are continuous. At the midplane, for symmetry reasons, the transverse stress vanishes $\partial_{\tilde{z}}\tilde{v}|_{1/2} = 0$.

The velocity field is now found by perturbatively solving eqs 19–21 in powers of ω; the lowest order allows the calculation of the loss modulus G'' and the first correction that of the storage modulus G'.

Up to first order in ω, eq 20 reads

$$\partial_{\tilde{z}}^2\tilde{v}^{(1)} = \frac{l(l-1)}{\tilde{z}^2}\tilde{v}^{(1)} + B^{(1)} \quad (22)$$

This allows the determination of the velocity profile in the adsorbed layers:

$$\tilde{v}^{(1)} = \frac{B^{(1)}}{(l+1)(2-l)}\left\{\tilde{z}^2 + \left[(1-l)\tilde{R}_f^{2-l} - \frac{(l+1)(2-l)}{2l}\tilde{R}_f^{1-l}\right]\tilde{z}^l\right\} \quad (23)$$

In the free solvent region the velocity is

$$\tilde{v}^{(1)} = B^{(1)}\left\{\frac{1}{2}(\tilde{z}^2 - \tilde{z}) - \frac{l-1}{2(l+1)}\tilde{R}_f^2 + \frac{l-1}{2l}\tilde{R}_f\right\} \quad (24)$$

These equations show an apparent singularity when $l = 2$. There is in fact no singularity, but logarithmic corrections appear in this limit.

From the velocity field, the pressure field can be calculated:

$$P(r) - P_\infty = -6i\omega\eta\gamma h_0 R\frac{1}{h^2(r)}\left[\frac{1}{2} + \frac{2(l-1)\ R_f}{l\quad h(r)} + O\left(\frac{R_f}{h}\right)^2\right] \quad (25)$$

One can then derive the total force on the plane by integration and then the loss modulus

$$G''(\omega) = \omega\eta\left[1 + \frac{2(l-1)R_f}{l\ \ h_0} + O\left(\frac{R_f}{h_0}\right)^2\right] \text{ for } \omega\tau_0 < 1 \quad (26)$$

This result has a simple interpretation; if $R_f < h_0$, the complex modulus can be expanded in powers of R_f/h_0. The zeroth-order term is the modulus of the pure solvent in the absence of polymer. The first-order term is contribution of the polymer, it is proportional to the viscous friction constant l, and it vanishes when $l = 1$ in the absence of polymer. The hydrodynamic force is identical to that of the steady compression experiment.

The expansion to second order of eq 21 for $\tilde{u}^{(1)}(z,\omega)$ gives:

$$\tilde{u}^{(1)} = -\int d\tilde{z}\left(\tilde{z}^3\int d\tilde{z}\frac{l(l-1)}{\tilde{z}^2}\tilde{v}^{(1)}\right) \quad (27)$$

which can be solved combining eq 23 and the boundary conditions.

By injecting the solution of the above equation in the second-order expansion of eq 20,

$$\partial_{\tilde{z}}^2\tilde{v}^{(2)} - \frac{l(l-1)}{\tilde{z}^2}\tilde{v}^{(2)} = -\frac{l(l-1)}{\tilde{z}^2}\omega\tau\tilde{u}^{(1)} + B^{(2)} \quad (28)$$

we find the second-order velocity profile.

In the pure solvent region:

$$\tilde{v}^{(2)} = \frac{B^{(2)}}{2}\left\{\tilde{z}^2 - \tilde{z} + \frac{(l-1)}{l}\tilde{R}_f - \frac{(l-1)}{(l+1)}\tilde{R}_f^2\right\} - i\omega\tau B^{(1)}\frac{l(l-1)^2}{(l+1)(l-2)}\left\{\frac{1}{8l}\tilde{R}_f^4 - \frac{(2l+7)}{10(l+1)(l+4)}\tilde{R}_f^5\right\} \quad (29)$$

In the adsorbed polymer layers:

$$\tilde{v}^{(2)} = \frac{B^{(2)}}{(l+1)(l-2)}\left\{\left((l-1)\tilde{R}_f^{2-l} - \frac{(l+1)(l-2)}{2l}\tilde{R}_f^{1-l}\right)\tilde{z}^l - \tilde{z}^2\right\} - i\omega\tau B^{(1)}\frac{l(l-1)^2}{(l+1)(l-2)}\left\{\frac{(l+1)(l-2)}{8(l-1)(l+3)(l-4)}\tilde{z}^4 - \frac{l}{5(l+4)(l-5)}\tilde{z}^5 - \left\{\frac{(l-2)(l+6)}{12l(l+3)(l-4)}\tilde{R}_f^{4-l} - \frac{(l+7)(l-2)}{6(l+1)(l+4)(l-5)}\tilde{R}_f^{5-l}\right\}\tilde{z}^l + \frac{1}{6(l-1)(l+1)(l+3)} \times \left(\frac{(l+1)(l-2)}{2}\tilde{R}_f^{1-l} - l(l-1)\tilde{R}_f^{2-l}\right)\tilde{z}^{(l+3)}\right\} \quad (30)$$

This expression is rather complicated, so we have plotted the second-order velocity profile for various values of the friction parameter l in Figure 1.

By integration of the velocity profile, the pressure and then the force between the sphere and the plane can be calculated. This force gives the elastic contribution to the complex modulus

$$G'(\omega) = \eta\omega^2\tau_0\left(\frac{(l-1)^2}{4(l+1)(l+3)}\right)\left\{\frac{R_f^4}{h_0^4} + O\left(\frac{R_f}{h_0}\right)^5\right\} \propto \frac{\omega^2 R_f^4}{h_0} \text{ for } \omega\tau_0 < 1 \quad (31)$$

In this expression, $\tau_0 = \eta h_0^3/\alpha k_B T$ is the Zimm relaxation time of a polymer solution with a correlation length h_0.

The frequency dependence of the elastic modulus ($\simeq\omega^2$) at low frequencies is the standard variation for a Maxwell viscoelastic fluid. An interesting point is the $R_f^4 \simeq N^{12/5}$ dependence of the storage modulus, which could be checked experimentally.

This molecular weight dependence can be obtained via the simple following argument. We consider the solution, in the gap of the surface force apparatus as a Maxwell fluid. In the terminal zone, at low frequency, the real and imaginary parts of the complex modulus are related by $G'(\omega)/G''(\omega) = \omega\tau$ where τ is the viscoelastic relaxation time. Our result for the polymer contribution to the loss modulus eq 26 is $G''_p = \omega\eta(R_f/h_0)$. This gives a storage modulus $G' = \omega^2\eta\tau(R_f/h_0)$. If we now choose as the relaxation time, the relaxation time of the large loops with a size of order R_f, $\tau(R_f) \propto \eta R_f^3/k_B T$, we obtain

$$G'(\omega) = \omega^2\eta^2\frac{R_f^4}{k_B T h_0} = \frac{\omega^2\eta^2 R_f^4}{E_0\, h_0^4} \quad (32)$$

which is the same result as eq 31, up to a numerical factor which depends on the friction coefficient l. This simple argument emphasizes the fact that at low frequency, the effect of the polymer on the viscoelasticity of the fluid in the gap of the surface force apparatus is dominated by the large loops of size R_f as already found for the effective hydrodynamic thickness of the layers.

C. Viscous and Elastic Normal Stresses. So far, we have only considered the contribution to the force between plates due to the pressure gradient. We can now check that the contribution of the normal viscous stress and of the normal elastic stress of the polymer network are negligible. The normal velocity gradient $\partial_z v_z$ can be calculated from the continuity equation (eq 9); it is independent of the radius of sphere. The normal viscous stress is also independent of the sphere radius and upon integration it gives a contribution to the force between the sphere and the plane proportional to the radius of the sphere. This is much smaller than the dynamic force calculated above which is proportional to the square of the radius. Similarly, the normal strain $\partial_z u_z$ can be calculated from the z-component of eq 6. It is independent of the sphere radius and the normal elastic force increases also linearly with R. In the limit of zero frequency, the hydrodynamic force vanishes ($G' = G'' = 0$) and the elastic force becomes measurable. In the very low frequency limit the elastic modulus reaches a finite value given by the static forces.

The frequency limit above which static forces can be neglected can be obtained by comparison of the static and dynamic (Reynolds) forces; the order of magnitude of these forces are:

$$F_{stat} \sim \int (E(z)\partial_z u_z)2\pi R dh \sim \frac{h_B T}{h^3} R h\gamma \quad (33)$$

$$F_{dyn} \sim \eta R^2\dot{\gamma}$$

The static force is small when

$$\omega\tau(h) > \frac{h}{R} \simeq 10^{-8} \quad (34)$$

which is not very restrictive.

Similarly, we can determine the frequency range where the Poisson ratio can be approximated by zero as done in eq 6. In general, the force per unit volume associated to a deformation of an isotropic body can be written as:[14]

$$f_i = \partial_j\sigma_{ij} = E\nabla^2\mathbf{u}_i + \lambda\partial_i\nabla\mathbf{u} \quad (35)$$

where σ_{ij} is the stress tensor and E and λ are the relevant elastic moduli that for simplicity we consider here as constants (this is sufficient to calculate orders of magnitude). The extra force per unit volume in the radial direction is then

$$\lambda\partial_r\left(\frac{1}{r}\partial_r(ru_r) + \partial_z u_z\right) \quad (36)$$

The first term involves a second derivative with respect to the radial coordinate and can be neglected within the framework of the lubrication approximation if the two elastic moduli are of the same order of magnitude. The second term can be compared directly to the Brinkman friction force $(\eta/\xi^2)v_r$. Using the fact that the deformation is $\partial_z u_z \sim \gamma$ and that the radial velocity is $v_r \sim \dot{\gamma}a$ where $a = \sqrt{Rh}$ is the characteristic radial length, we find that the Poisson ratio can be approximated by zero if the frequency satisfies the same inequality given by eq 34.

4. Weakly Overlapping Polymer Layers

We now study the case where the two polymer layers overlap around the center of the surface force apparatus. Even in this central region, we assume that the overlap is weak enough that the concentration profile is not perturbed and is still given by the self-similar law on each plate. The case of strongly overlapping layers is well described by the constant concentration model studied by Fredrickson and Pincus.

The geometry is sketeched in Figure 2. There are two different regions: in the central part ($r < r_l$), the adsorbed layers overlap and $h(r) < h_l = 2R_f$. In the outer region ($r > r_l$), the two layers do not overlap and there is a free solvent layer in the middle of the gap.

In the outer region, the boundary conditions for the flow are the same as in section 3. In the central region the

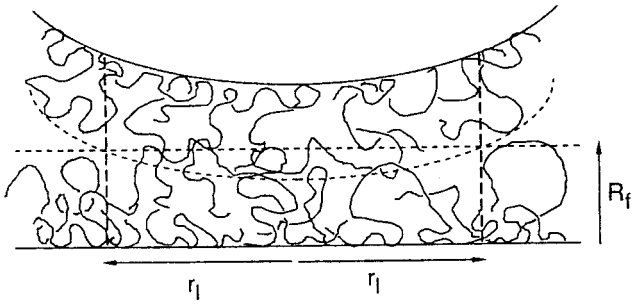

Figure 2. Weakly overlapping adsorbed layers: $R_f < h_0/2$. Two different regions have to be defined on each side of the limit where the two layers separate: $h_l = 2R_f$. In the *inner* region ($h < h_l$) there is no pure solvent region inside the gap. The *outer* region ($h > h_l$) is equivalent to the geometry sketched in Figure 1.

boundary conditions at $z = R_F$ are replaced by boundary conditions at the midplane imposed by the symmetry $\partial_z u|_{1/2} = 0$, $\partial_z v|_{1/2} = 0$. In the following, the variables in the central region are indexed by $<$ and the variables in the outer region by $>$. We first calculate the loss modulus G'' by perturbatively solving eqs 5 and 6 to lowest order in ω; the storage modulus G' is then obtained from the next order.

A. Loss Modulus. At lowest order in ω, the velocity profile in the central region ($h(r) < h_l = 2R_f$) is given by

$$\tilde{v}_r^{(1)}|_< = \frac{B^{(1)}|_<}{(l+1)(2-l)}\left(\tilde{z}^2 - \frac{2^{l-1}}{l}\tilde{z}^l\right) \tag{37}$$

The pressure gradient can be calculated from the incompressibility condition (eq 9):

$$\partial_r P^{(1)}|_< = i\omega\eta\gamma h_0 \frac{r}{h(r)^3}\frac{6l(l+1)^2}{l+3} \tag{38}$$

In the outer region the pressure gradient is the same as that obtained in section 3 for nonoverlapping layers:

$$\partial_r P^{(1)}|_> = 6i\omega\eta\gamma h_0 \frac{r}{h(r)^3}\left[1 + a\left(\frac{R_F}{h(r)}\right) + b\left(\frac{R_F}{h(r)}\right)^2 + c\left(\frac{R_F}{h(r)}\right)^3\right]^{-1} \tag{39}$$

where a, b, and c are functions of the friction parameter l

$$a = \frac{6(l-1)}{l} \qquad b = \frac{12(l-1)}{(l+1)} \qquad c = \frac{8l(l-1)}{(l+1)^2} \tag{40}$$

The hydrodynamic force can be split into two components coming from the central and outer regions, respectively.

$$F^{(1)} = F^{(1)}|_< + F^{(1)}|_> \tag{41}$$

The pressure at very large radius is equal to the atmospheric pressure, so the pressure field in the outer region is directly obtained by integration of the pressure gradient. A further integration gives the contribution to the hydrodynamic force:

$$F^{(1)}|_> = -12\pi i\omega\eta\gamma h_0 \frac{R^2}{R_f} f(l) \tag{42}$$

where $f(l)$ is a dimensionless number depending only on the friction parameter l:

$$f(l) = \int_2^\infty \frac{x-2}{x^3 + ax^2 + bx + c}\,dx \tag{43}$$

In the central region, the pressure is calculated from the pressure gradient by imposing its continuity as $r = r_l$; the contribution to the force from the central region is

$$F^{(1)}|_< = -6\pi\gamma i\omega\eta R^2\left(\frac{l(l+1)^2}{(l+3)} + \frac{h_0}{R_f}\left(4g(l) - \frac{l(l+1)^2}{(l+3)}\right) + \frac{h_0^2}{R_f^2}\left(\frac{l(l+1)^2}{(l+3)} - 3g(l)\right)\right) \tag{44}$$

where

$$g(l) = \int_2^\infty \frac{dx}{x^3 + ax^2 + bx + c} \tag{45}$$

Summing these two contributions, we obtain the viscous dissipation modulus:

$$G''(\omega) = \omega\eta\left\{\frac{l(l+1)^2}{l+3} + \alpha(l)\frac{h_0}{R_f} + \beta(l)\frac{h_0^2}{R_f^2}\right\} \tag{46}$$

where

$$\alpha(l) = 4g(l) - \frac{l(l+1)^2}{l+3} + 2f(l), \quad \beta(l) = \frac{l(l+1)^2}{4(l+3)} - 2g(l) \tag{47}$$

The functions $\alpha(l)$ and $\beta(l)$ are plotted as a function of l in Figure 3. The figure also displays the variation of the effective viscosity $G''(\omega,l)/\omega$. The coefficients α and β vanish when $l = 1$ in the absence of polymer and the loss

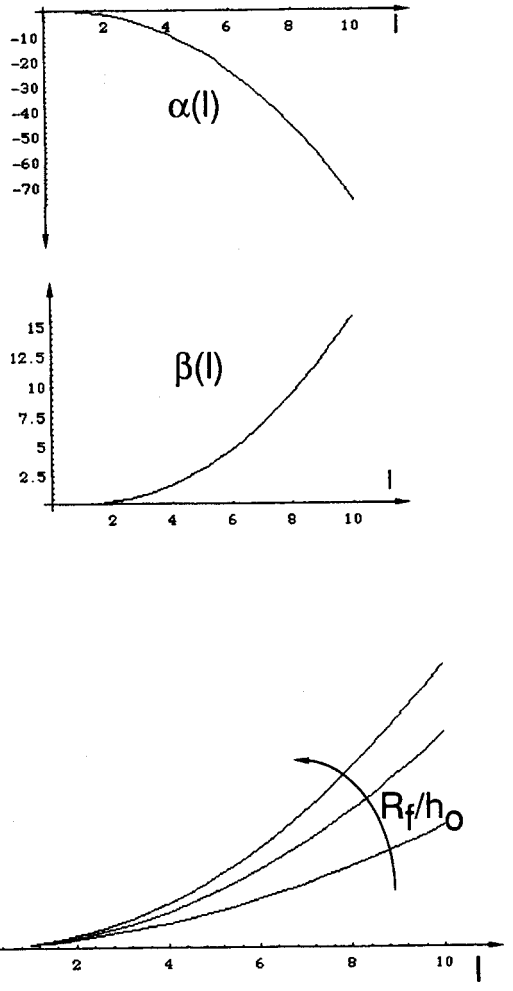

Figure 3. Loss modulus for weakly overlapping polymer layers as described by eq 44. $\alpha(l)$ and $\beta(l)$ are friction dependent functions given by eq 45. The ratio $G''(\omega)/\omega\eta$ represents the effective viscosity of the solution; it is plotted for three different distances h_0: $R_f/h_0 = 1$, $R_f/h_0 = 2$, $R_f/h_0 = 5$.

modulus G'' is equal to the pure solvent value given by Reynolds lubrication theory eq 1. G'' also increases with l, i.e. when the friction between polymer and solvent increases. The dominant contribution to the hydrodynamic force comes from the central region where the two adsorbed polymer regions overlap.

B. Storage Modulus. The storage modulus is obtained from an expansion to second order in ω. In the outer region where the two polymer layers do not overlap ($h(r) > h_l$), the velocity profile is the same as the one derived in section 3 (eqs 29 and 30). In the central region, where the two layers overlap, the velocity profile is found by substituting $^1/_2$ to R_f in eq 30, which corresponds to a change in the boundary conditions. After integration of the velocity, we obtain the pressure gradient using the incompressibility condition eq 9:

In the inner region $h(r) > h_l$:

$$\partial_r P^{(2)}|_> = -6\phi\left(l, \frac{h(r)}{R_f}\right)\omega^2\eta\gamma\frac{\tau_0}{h_0^2}r \qquad (48)$$

In the outer region: $h(r) < h_l$

$$\partial_r P^{(2)}|_< = -6\Theta(l)\omega^2\eta\gamma\frac{\tau_0}{h_0^2}r \qquad (49)$$

where $\phi(l, x)$ and $\Theta(l)$ are rather complicated functions of the friction parameter l, and of the dimensionless variable $x = h(r)/R_f$ that will not be displayed explicitly.

The elastic modulus is then obtained following the same procedure as in the previous section:

$$G'(\omega) = 2\omega^2\eta\tau_0\left[2\frac{R_f^2}{h_0^2}\{2\Theta(l) + 2\Phi(l) + \psi(l)\} - \frac{R_f}{h_0}\{2\Theta(l) + \Phi(l)\} + \frac{1}{2}\Theta(l)\right] \qquad (50)$$

where $\Phi(l)$, and $\psi(l)$ are two l-dependent functions defined by the integrals:

$$\Phi(l) = \int_2^\infty \phi(l, x)\mathrm{d}x \quad \textit{and} \quad \psi(l) = \int_2^\infty (x-2)\phi(l, x)\mathrm{d}x \qquad (51)$$

These integrations were performed numerically and the results are shown in Figure 4. As expected, all the l-dependent factors in the expression of G' increase monotonically and vanish for $l = 1$, in the absence of polymers between the surfaces. The adsorbed polymer in this case also has a purely elastic response and the storage modulus is proportional to ω^2. The important result is the variation with molecular weight: G' is proportional to R_f^2 or to $N^{6/5}$. As for the dissipative response, we can see in Figure 4 that G' is dominated by the central region (represented by $\Theta(l)$).

5. Periodic Compression at High Frequency

In the low frequency limit, the adsorbed polymer chains act as an elastic porous medium that has been described by the Brinkman approximation. At higher frequency, the internal modes of the loops forming the adsorbed layers are excited and the Brinkman approximation is not valid. This high frequency limit is now discussed briefly.

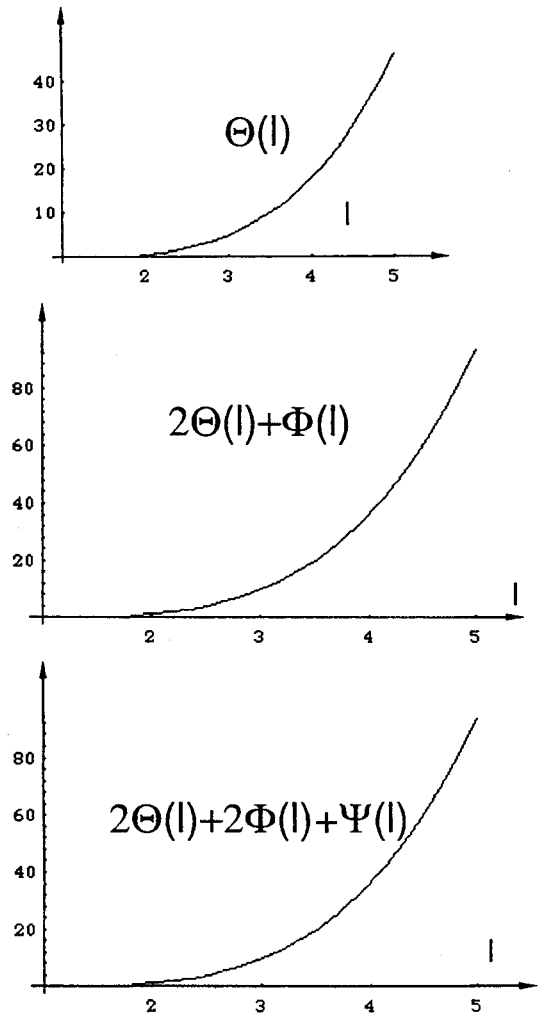

Figure 4. l-Dependent coefficients of the storage modulus $G'(\omega)$ obtained by numerical integration of (eq 49). We observe the expected monotonical behavior and the vanishing values for $l = 1$ (no friction) of the functions $\{\Theta(l)\}$, $\{2\Theta(l) + \Phi(l)\}$, and $\{2\Theta(l) + 2\Phi(l) + 2\Phi(l) + \Psi(l)\}$.

At a finite frequency ω, all the internal modes of the chains, with a relaxation time τ so that $\omega\tau > 1$, are excited. For a portion of chain of size ξ, the typical relaxation time is given by the Zimm formula $\tau(\xi) = \eta\xi^3/kT$. We define the length scale ξ_ω such that $\omega\tau(\xi_\omega) = 1$

$$\xi_\omega \propto \left(\frac{k_B T}{\eta\omega}\right)^{1/3} \qquad (52)$$

For all sizes ξ smaller than ξ_ω, in the vicinity of the adsorbing surfaces, $\omega\tau < 1$ and the Brinkman approximation can still be used. For sizes larger than ξ_ω, at a distance from the adsorbing surfaces $z > \xi_\omega$, we group the monomers into dynamic blobs of size ξ_ω each containing $g_\omega = (\xi_\omega/a)^{5/3} \propto (k_B T/\eta\omega)^{5/9}$ monomers. A sketch of the blob solution in the adsorbed layers is given on Figure 5. From the hydrodynamic point of view, the blobs can be considered as independent and the friction on each blob is given by Stokes law. The effective friction per monomer is thus $f_m = 6\pi\eta\xi_\omega/g_\omega$. In the limit where the size of the dynamic blob is equal to the local correlation length of the solution, this friction crosses over smoothly toward the effective friction on a monomer given by the Brinkman approximation using the usual scaling laws for $g(\xi)$ and $c(\xi)$.

The equation of motion of the polymer network is obtained by writing a balance between the solvent friction

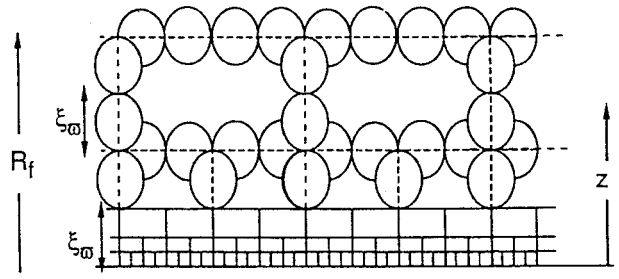

Figure 5. Schematic blob model of an adsorbed polymer layer under periodic compression at high frequency. A characteristic length ξ_ω is associated at each frequency ω via the Zimm relaxation time $\omega\tau(\xi_\omega) = 1$. For $z < \xi_\omega$, $\omega\tau(z) < 1$, and the self-similar profile $\xi(z) \propto z$ is still valid. For $\xi_\omega < z < R_f$, the layer is equivalent to a solution of blob of constant size ξ_ω. For $R_f < z < h/2$, there is only solvent in the solution.

and the elastic stress

$$\nabla\left(\frac{E(\omega)}{c(z)}\nabla\mathbf{u}\right) = -f_m(\omega)(\mathbf{v} - \dot{\mathbf{u}}) \tag{53}$$

In this equation, $E(\omega)$ is the local frequency-dependent elastic modulus of the adsorbed layer. Equation 53 is a local balance of forces at the scale of a dynamic blob; it must thus be independent of z or of the correlation length $\xi(z)$. In order to find the variation of the elastic modulus with frequency, we use a scaling argument. We write the elastic modulus as:

$$E(\omega) = \frac{k_B T c(\xi(z))}{g(\xi(z))} f[\omega\tau(\xi(z))] \tag{54}$$

The scaling function f is of order one in the limit where $\omega\tau < 1$. In the high frequency limit, it behaves as a power law. Imposing that $E(\omega)/c(z)$ is independent of $\xi(z)$, we obtain $E(\omega) = k_B T c(z)\omega^{5/9}$. This result was also derived by Doi and Edwards using a slightly different argument.[11]

Following the lines of section 2, the force balance on the adsorbed polymer can be written as

$$\partial_z^2 u_r = -\frac{1}{\omega\xi_\omega^2}(v_r - \dot{u}_r) \tag{55}$$

Within the lubrication approximation, the equation of motion of the solvent is written as:

$$\partial_z^2 v_r = \frac{1}{\xi_\omega^{2/3} z^{4/3}}(v_r - \dot{u}_r) + \frac{\partial_r P}{\eta} \tag{56}$$

The complex modulus $G(\omega)$ of the adsorbed polymer in the surface force apparatus can in principle be obtained along the same lines as above from eqs 55 and 56. We do not give a complete derivation here but rather use a simple scaling argument.

We first consider the case where the two adsorbed layers are not overlapping $h_0 > 2R_F$. In the high frequency limit, the dynamic blob size ξ_ω is smaller than the Flory radius R_f of the largest loops and we divide the gap between the sphere and the plane into three regions. Close to the adsorbing surface $z < \xi_\omega$, the Brinkman equation can be used and the velocity profile is calculated using the two fluids model of section 2. At intermediate distances $\xi_\omega < z < R_f$ we use the dynamic blob model and eqs 55 and 56. In the center of the gap there is no polymer and the velocity is governed by the usual Stokes equation.

In the intermediate range, the relative velocity between polymer and solvent satisfies

$$\partial_z^2(\tilde{v}_r - i\omega\tau\tilde{u}_r) = \frac{1}{\xi_\omega^2}\left(i + \left(\frac{\xi_\omega}{z}\right)^{4/3}\right)(\tilde{v}_r - i\omega\tau\tilde{u}_r) + \frac{\partial_r P}{\eta} \tag{57}$$

This equation can be solved in the limit $z \gg \xi_\omega$ and gives the velocity profile in the intermediate region

$$v_\omega = \frac{1}{2}B\{z^2 - z + C\} - BC' i\xi_\omega^{4/3}\frac{e^{-\sqrt{i}\frac{z}{\xi_\omega}}}{z^{4/3}} \tag{58}$$

where $B = \partial_r P/\eta$ measures the pressure gradient and C and C' are integration constants that could be determined from a matching of this velocity with the velocity profile in the inner region. This matching is rather complicated and will not be done explicitly here.

The first term on the right hand side is the same as the velocity profile in the central region where there is no polymer. The second term is due to the friction between polymer and solvent; it decays exponentially over the dynamic blob size ξ_ω and is vanishingly small over much of the intermediate region. In most of the intermediate region, the influence of the polymer is negligible and the mechanical behavior of the surface force apparatus is the same as that of two surfaces coated with polymer layers of thickness ξ_ω. It is clear from the representation of the blob model of Figure 5 that the friction is drastically reduced at high frequency; it becomes negligible in eq 56 and the velocity profile is not affected by the polymer in the intermediate region.

The complex modulus is then obtained at the level of scaling laws by replacing R_f by ξ_ω in eqs 26 and 31. We obtain

$$G'(\omega) \simeq \eta\tau_0^{-1/3}\omega^{2/3}$$

$$G''(\omega) = \omega\eta + \eta\tau_0^{-1/3}\omega^{2/3} \tag{59}$$

In the case where the two adsorbed polymer layers overlap ($R_f > h_0$), we use the same kind of scaling argument. If $h_0 < \xi_\omega < R_f$ or $\omega_f = \tau(R_f)^{-1} < \omega < \omega_0 = \tau_0^{-1}$, the two layers of thickness ξ_ω on the sphere and the plane overlap and we find the complex modulus from the results of section 4 (eqs 50 and 46) by replacing R_f by ξ_ω

$$G'(\omega) = \eta\tau_0^{1/3}\omega^{4/3}$$

$$G''(\omega) = \omega\eta\frac{l(l+1)^2}{l+3} + \eta\tau_0^{1/3}\omega^{4/3} \tag{60}$$

At even larger frequency ($\omega > \omega_0$) the layers of size ξ_ω on the two surfaces no longer overlap and the complex modulus is given by eq 59. It is easily checked that the modulus is continuous when $\omega = \omega_0$ and crosses over smoothly to the low frequency results when $\omega = \omega_f$.

6. Discussion

We have analyzed the viscoelastic behavior of adsorbed polymer layers in an idealized surface force apparatus made of a sphere and a plane. Two types of experiments have been considered, a steady-state experiment where the distance between the sphere and the plane decreases with a small constant velocity, and a finite frequency experiment where the distance has small amplitude oscillations.

In the steady-state experiment, when the two adsorbed polymer layers do not overlap, each polymer layer has a hydrodynamic thickness e_H of the order of the size of the largest loops R_f, and the effect of the polymer is equivalent

to an effective reduction of the gap between the sphere and the plane by $2e_H$ in agreement with a previous result of de Gennes.

In the finite frequency experiment, there is a finite elastic modulus at zero frequency when the two layers overlap. If this plateau value is substracted off, the complex modulus has at low frequency a Maxwell-like behavior, the real part G' is proportional to ω^2 and the imaginary part G'' varies linearly with ω. When the two adsorbed polymer layers do not overlap, the effect of the polymer on the loss modulus is small and the imaginary modulus is small and is proportional to R_f^4. This prediction could perhaps be checked experimentally. When the two layers overlap, the contribution of the polymer to the loss modulus due to the friction between polymer and solvent is of the same order as the pure solvent contribution. The elastic modulus is proportional to R_f^2. This Maxwell regime is expected until a pulsation ω_f of the order of the inverse Zimm relaxation time of the chains. At higher frequency we predict a contribution of the polymer to the complex modulus proportional to $(i\omega)^{2/3}$ in the nonoverlapping case. In the overlapping case there are two frequency regimes if $\omega_f < \omega < \omega_0$ where ω_0 is of the order of the inverse relaxation time of a loop with a size h_0 (the minimum distance between the sphere and the plane), the contribution of the polymer to the loss modulus is of the same order as the pure solvent contribution and the elastic modulus varies as $\omega^{4/3}$. At higher frequency we find the same result as in the nonoverlapping case.

The hydrodynamic model used to describe the adsorbed polymer layers is the two fluid models. At low frequency we have used the so-called Brinkman approximation to describe the friction between polymer and solvent; at higher frequency we have constructed a blob model. It will be interesting to compare these rather rough models to a hydrodynamic model based on first principles such as the one currently worked out by Wu and Cates.[15] At high frequency, inertial effects of the solvent that govern the diffusion of vorticity also become important; they can, however, be neglected as long as the distance between the sphere and the plane is smaller than $(\eta/\rho\omega)^{1/2}$ where ρ is the solvent density. This constraint is always satisfied in the relevant experimental frequency range.

It is interesting to compare our results with those obtained by Fredrickson and Pincus who studied a similar problem for a surface force apparatus where the two surfaces are coated with grafted polymer and not with adsorbed polymer. They studied only the low frequency limit and found a loss modulus varying linearly with frequency but an elastic modulus with an anomalous behavior $G' \simeq \omega^{13/11}$. This is due to the fact that for grafted polymer, the flow does not penetrate inside the polymer layer over the whole thickness but only over a very small part of the layer (with a size equal to the blob size).

Experiments have been performed in the geometry studied here by Pelletier et al. with, however, small differences. The polymer is not in a good solvent but in a θ solvent, the static force between the sphere and the plane is not monotonically repulsive but is attractive at large distances. The solution is not washed and replaced by pure solvent after the adsorption of polymer. In the case where the adsorbed polymer layers do not overlap, the gap does not contain pure solvent but a semidilute polymer solution. Nevertheless it is interesting to compare qualitatively our results with these experiments. At low frequency, a finite elastic modulus is measured only when the two layers overlap. After substraction of this plateau value, a Maxwell behavior is observed. At higher frequency, the complex modulus increases with a lower power of ω and seems to depend weakly on h_0, but the range of h_0 is rather small. The crossover between the low frequency and high frequency regimes occurs at around 10 Hz; this roughly agrees with estimates that can be made of ω_0 or ω_f ($\simeq$100 Hz). We hope that further experiments will allow a more quantitative comparison with our theoretical results.

Acknowledgment. We would like to thank J. P. Monfort and E. Pelletier (University of Pau) for useful discussions on their experiments that stimulated this work. We also benefitted from exchanges with M. Cates and D. Wu on the hydrodynamic properties of adsorbed polymer layers. We would like to acknowledge partial support from the C.N.R.S. through the program "*Forces de Surface*" (*GdR* 936).

References and Notes

(1) Israelachvili, J. N. *Intermolecular and Surface Forces*; Academic: London, 1985.
(2) Klein, J. In *Les Houches session XLVIII 1988-Liquids at Interfaces*; Charvolin, J., Joanny, J. F., Zinn-Justin, J., Eds.; Elvisier: Amsterdam, 1990.
(3) Klein, J. et al. *Macromolecules* **1993**, *26*, 5552.
(4) Reynolds, O. *Philos. Trans. R. Soc. London* **1886**, *157*, 177.
(5) Batchelor, G. K. *Introduction to Fluid Dynamics*; Cambridge University Press: Port Chester, NY, 1981.
(6) Pelletier, E.; Monfort, J. P.; Loubet, J. L.; Tonck, A.; Georges, J. M. *Macromolecules*, in press.
(7) Ferry, J. D. *Properties of Polymers*; John Wiley & Sons; New York, 1980.
(8) Fredrickson, G. H.; Pincus, P. *Langmuir* **1991**, *7*, 786.
(9) de Gennes, P. G. *Macromolecules* **1981**, *14*, 1637.
(10) de Gennes, P. G. *Scaling Concepts in Polymer Physics*; Cornell University Press: Ithaca, NY, 1978.
(11) Doi, M.; Edwards, S. F. *The Theory of Polymer Dynamics*; Clarendon Press: Oxford, 1986.
(12) Brinkmann, H. C. *App. Sci. Res.* **1947**, *A1*, 27.
(13) de Gennes, P. G. *Macromolecules* **1982**, *15*, 492.
(14) Landau, L. D.; Lifshitz, E. M. *Theory of Elasticity*; Pergamon Press; Oxford, 1981.
(15) Wu, D. T.; Cates, M. E. Unpublished.